Effect of cation addition on silica scale on glass surfaces

Hayashi, Shogo
TOTO Ltd.

Hatano, Shota
Department of Materials, Graduate School of Engineering, Kyushu University

Kobayashi, Tomoki
TOTO Ltd.

Saito, Noritaka
Department of Materials, Graduate School of Engineering, Kyushu University

他

出版情報：International Journal of Ceramic Engineering & Science. 6 (2), 2024-03. Wiley
バージョン：

Received: 16 September 2023 | Revised: 27 November 2023 | Accepted: 28 January 2024

DOI: 10.1002/ces2.10203

International Journal of Ceramic Engineering & Science

RESEARCH ARTICLE

Effect of cation addition on silica scale on glass surfaces

Shogo Hayashi[1] | **Shota Hatano**[2] | **Tomoki Kobayashi**[1] | **Noritaka Saito**[2] | **Kunihiko Nakashima**[2]

[1]TOTO Ltd., Kitakyushu, Japan

[2]Department of Materials, Graduate School of Engineering, Kyushu University, Fukuoka, Japan

Correspondence
Noritaka Saito, Department of Materials, Graduate School of Engineering, Kyushu University, 744, Motooka Nishi, Fukuoka 819-0395, Japan.
Email: saito.noritaka.655@m.kyushu-u.ac.jp

Abstract

Mineral components in tap water generally contaminate sanitary ware. In this study, various cations (Mg, Ca, and Al) were added to an aqueous solution containing silica to prevent water stains on sanitary ware. The particle size in the aqueous solution was measured and observed to increase for all cations. To create artificial water stains, a solution containing the cations and silica was dropped onto glass and allowed to dry. When these water stains were removed by sliding, the removal rate was higher for the water stains that contained the cations. This trend was attributed to the formation of precipitates owing to the reaction of silica with the added cations in the aqueous solution. The formation of these precipitates possibly increased the particle size and brittleness of water stains owing to their sparse structure. These findings provide insights into silica-scale removal, which can improve the cleanliness of sanitary ware and reduce the frequency of maintenance.

KEYWORDS

silica, surface, thin films

1 | INTRODUCTION

Toilets are an essential part of human hygiene, and their significance has been highlighted by various studies. Huuhtanen and Laukkanen[1] reported the importance of improving toilet hygiene in developing countries. Maintaining toilet hygiene is necessary to minimize the risk of pathogen transmission.[2] Inadequate toilet hygiene inflicts health hazards and decreases the number of tourists attracted to an area.[3] Therefore, toilet hygiene extends beyond the appearance and cleanliness of toilets and has become an issue with a high social impact.

Stains on sanitary ware originate from human metabolites. This problem has been addressed by various research approaches and sanitary-ware manufacturing techniques. For example, Wang et al.[4] reported that spraying polydimethylsiloxane on sanitary ware enhances its surface lubricity and resistance to stains caused by human metabolites.

In addition to human metabolites, other major sources of sanitary contamination include water stains. Sanitary ware is typically cleaned using tap water, which contains many mineral components such as Si, Ca, and Mg; water stains are formed when these components adhere to the sanitary ware surface.[5] Tap water is used in toilets and also in faucets and sinks in ordinary households. Therefore, water staining is inevitable in everyday life.

McCartney et al.[6] observed that water staining is caused by the aggregation and polymerization of silicic acid in water that is used in heat exchangers of geothermal power

plants; these polymers adhere to and accumulate on solid surfaces and have become a considerable challenge in the industry. Various approaches involving silica-scale inhibitors have been proposed to prevent industrial water staining.

Neofotistou and Demadis[7] examined the applicability of polyamide-based dendrimers as silica-scale inhibitors. Amjad and Yorke[8] reported that cation-based copolymers are effective silica scale inhibitors. Harrar et al.[9] demonstrated the effectiveness of cation-based copolymers and surfactants as silica-scale inhibitors for geothermal power applications. Spinthaki et al.[10] used dispersants and inhibitors to prevent silica particles from bonding to each other. Gallup[11] investigated the use of several commercial organic additives as anti-scaling agents for silica. Gill[12] demonstrated that acrylic acid/2-acrylamido-2-methylpropylsulfonic acid copolymers effectively inhibit silica scaling at high concentrations of silica solutions.

These studies reveal that silica-scale inhibitors effectively reduce silica deposition. However, silica-scale inhibition on glass surfaces, such as in sanitary ware, has not been examined thus far. Previous studies have primarily focused on large heat exchangers, whereas applications involving small amounts of water (e.g., commercial sanitary ware) have not been considered.

In this study, we examine the removal of water stains via the addition of Al, which has been reported to precipitate silica, and cations such as Mg and Ca, which are present in tap water. Moreover, the phenomena occurring in solutions containing monomeric silica are verified by measuring the particle size and zeta potential when the solutions are dropped onto a glass substrate-like surface.

2 | EXPERIMENTAL PROCEDURE

2.1 | Sample preparation

Because tap water generally contains varying amounts of silica, we prepared an artificial solution containing a specific amount of silica. In this study, aqueous solutions containing Ca, Mg, and Al cations were prepared for artificial water-stain formation.

Initially, 1.0 g of anhydrous silicic acid (SiO_2) and 4.0 g of sodium carbonate (Na_2CO_3) were melted at a high temperature (1200°C) in a Pt dish. The molten liquid was diluted with distilled water to prepare 1 L of silica-containing water.

In this study, the silica concentration was maintained at 200 ppm, and 0, 5, and 10 ppm of Al was added using an aluminum nitrate solution (Sigma–Aldrich). Calcium was added as calcium nitrate (Fujifilm Wako Pure Chemicals Co., Ltd.). Magnesium was added as magnesium nitrate (Fujifilm Wako Pure Chemical Co., Ltd.). Finally, nitric acid (Sigma–Aldrich) was used to adjust the pH of the solution to 2, 4, or 7. Fifty microliters of each prepared silica-containing aqueous solution was dropped onto a glass substrate from a height of 2 mm. Subsequently, the substrate was placed in a constant temperature and humidity chamber (55°C, 50%) to enable the water droplets to dry and form a silica scale. To set the concentrations of Mg and Ca, we referred to documents of the Japanese Ministry of Education, Culture, Sports, Science, and Technology reporting water supply components[13]; the maximum values of Ca and Mg in Japanese tap water are 84.8 and 20.0 ppm, respectively (converted from mg/100 mL). Four levels were selected to alternate the parameters between the following values: Ca: 40 and 80 ppm; Mg: 9.7 and 19.4 ppm.

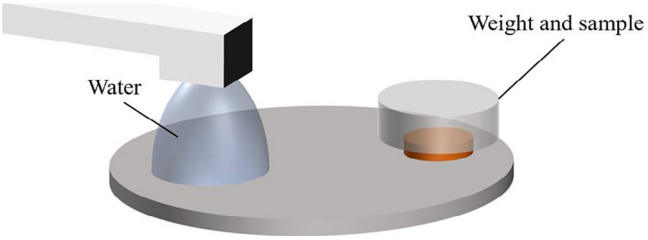

FIGURE 1 Experimental method of sliding test.

2.2 | Sliding test

To quantify the silica-scale removal rate, sliding tests were performed using a rotary grinder (Figure 1). The rotation speed during sliding was 10 rpm; the pressure and water volume were 7.65 kPa and 11.5 mL/s, respectively. Each sample was tested for 0, 60, 120, 180, 240, and 300 s. After sliding, the volume was measured using a color three-dimensional (3D) laser microscope (VK-9700, Keyence Japan Corp.). Multiple images of the entire water stain were captured, and the image data were combined using an image combination application (VK-H1J1, Keyence Japan Corp.) to obtain 3D information of the entire water stain. The resulting image was analyzed using the volume and surface area measurement mode of a shape analysis application (VK-H1A1, Keyence Japan Corp.) to directly determine the volume of the water stain.

2.3 | Zeta potential measurement

The zeta potential indicates whether the particles constituting the system are electrostatically positively or negatively charged. If the particle system is positively

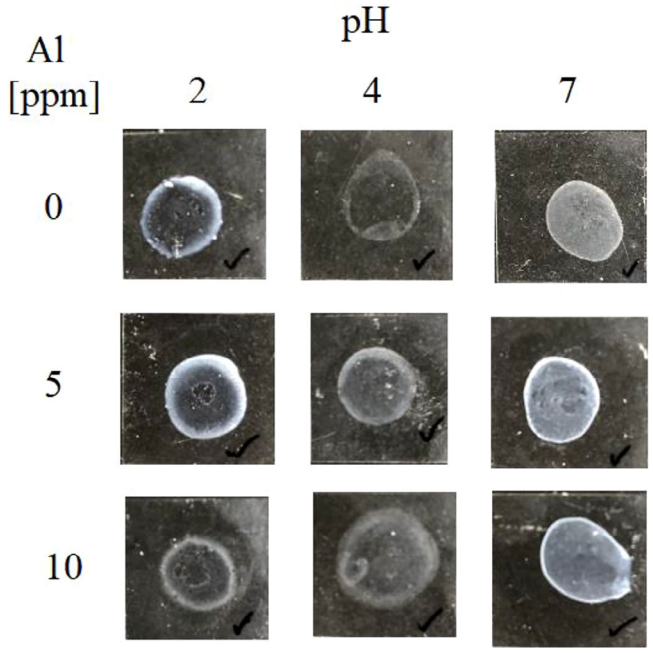

FIGURE 2 Shape change after droplet drying at various pH and Al concentrations.

or negatively charged, repulsion between the particles is expected to occur. The zeta potential was measured using a Zetasizer Zero instrument (Spectris Co., Ltd.).

2.4 | Particle size measurement

Employing the same equipment and conditions described in Section 2.3, the particle size distribution was determined through dynamic light scattering. In this method, a laser beam was initially irradiated on particles in Brownian motion. The particle size was evaluated by measuring the scattered light corresponding to the speed of the Brownian motion of the particles.

3 | RESULTS AND DISCUSSION

3.1 | Effect of Al addition on zeta potential and particle size

Figure 2 shows an optical micrograph of the silica scale and photographs of the samples for which the pH of the solution was varied between 2, 4, and 7, and the concentration of added Al ions was varied between 0, 5, and 10 ppm. A water stain was formed on each sample after the silica-containing aqueous solution was dried. A coffee-ring effect[14] was observed at all pH values and Al concentrations. In previous studies, particle aggregation was observed as the zeta potential approached

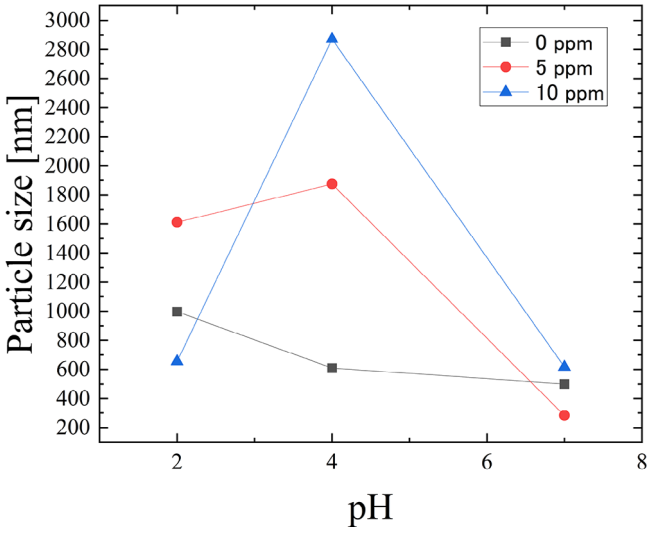

FIGURE 3 Particle size at different Al concentrations.

zero.[15,16] According to these studies, coffee rings were formed or deposited uniformly when the zeta potential was below 20 mV. Moreover, particle agglomeration via the coffee-ring effect can be explained using the Derjaguin–Landau–Verwey–Overbeek (DLVO) theory. Based on this theory, the particles are expected to be uniformly deposited inside the coffee ring as the zeta potential approaches zero; however, this was not observed in the present study.

Figure 3 shows the particle size measurements in silica-containing water when Al was added; peaks are observed at both 10 and 5 ppm of Al at pH 4. At pH 4, the particle size increased with increasing Al concentration up to 10 ppm. Sheikholeslami et al.[17] observed that the addition of sodium aluminate to an aqueous solution containing silica decreased the silica concentration, because silicic acid was flocculated and precipitated in this solution. Moreover, they reported that the addition of Al resulted in water softening via the following reaction:

$$Al_2SiO_5(OH)_4 + 6H^+ \Leftrightarrow 2Al^{3+} + 2Si(OH)_4 + H_2O \quad (1)$$

Equation (1) indicates that Al ions react with silicic acid to precipitate kaolinite; this phenomenon is ascribed to the substitution of Si with Al. Similarly, Tokoro et al.[18] reported that co-precipitation occurred by the intervention of Al ions in aqueous solutions containing silica; when Na and Al were added to a system of silicate and water, and the initial Si/Al molar ratio was greater than 2, poorly crystallized kaolinite precipitated according to Equation (1).

Figure 4 presents the zeta potentials measured upon adding Al. The point at which the zeta potential became zero, that is, the equipotential point, changed under the influence of Al. The addition of 5 ppm of Al decreased the zeta potential to 15.9 mV at pH 4. Moreover, at pH 4, the addition of Al was expected to result in stronger

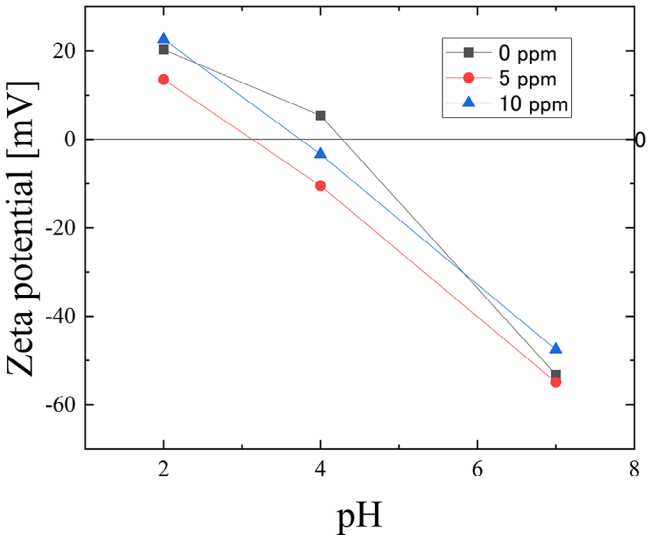

FIGURE 4 Zeta potential at different Al concentrations.

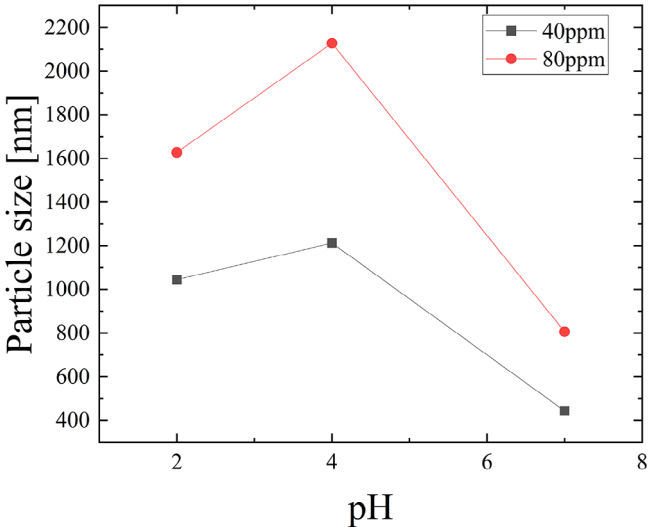

FIGURE 5 Particle size at different Ca concentrations.

aggregation between the particles, considering the decreasing zeta potential. When the zeta potential approached zero, cohesive forces were predominant. In contrast, when the zeta potential moved to positive or negative values, the electrostatic repulsive forces between the particles became predominant. Furthermore, a strong relationship was observed between the coffee-ring effect, which results in water stains, and the DLVO theory.[15,16] The particle size distribution results (Figure 3) suggest that agglomeration according to the DLVO theory occurs at the point of electrical neutrality within the pH range of 3–4. In this region, Al-ion addition demonstrated the highest agglomeration effect, and the average particle size was expected to be the largest.

Therefore, in this study, Al-ion addition presents the possibility of the flocculation and precipitation of silica in an aqueous solution. The precipitation mechanism is indicative of water softening, suggesting that the precipitate contains kaolinite.

3.2 | Effect of Ca addition on zeta potential and particle size

Figure 5 presents the particle size as a function of pH for different levels of Ca addition. The particle size increased at pH 4 when the amount of added Ca was increased from 40 to 80 ppm. This increase in the particle size was attributed to the agglomeration and precipitation of silica in the aqueous solution.

Silica removal by the addition of Ca and Mg ions has been previously investigated.[19,20] In these studies, the amount of total dissolved solids (TDS) was found to influence silica removal via the addition of Ca and Mg. TDS

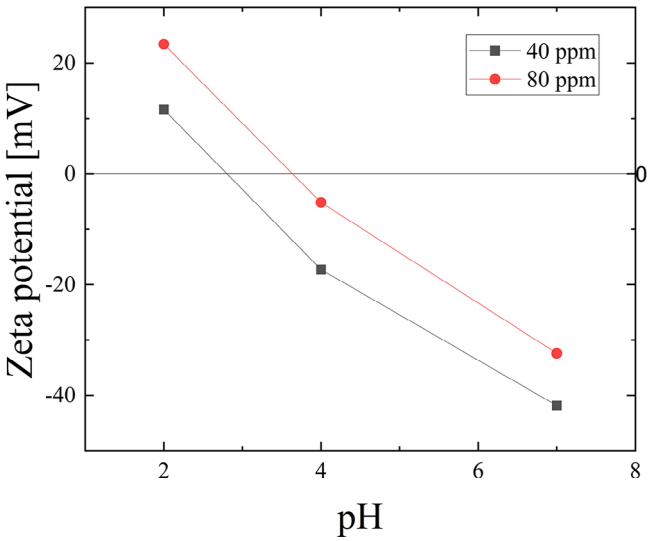

FIGURE 6 Zeta potential at different Ca concentrations.

indicates the total amount of inorganic salts dissolved in water containing Ca and Mg, and these values affect silica-scale removal.

Furthermore, silica-scale formation was reported to be inhibited by co-precipitation. Particularly, the TDS value was substantially increased because the Ca concentration increased during the study. A higher TDS value implies stronger silica scale inhibition, resulting in co-precipitation and the formation of silica-containing flocs, which increases the average particle size.

Figure 6 shows the increase in the zeta potential with the increasing addition of Ca. Accordingly, the equipotential point is shifted. The equipotential point is observed at approximately −3.7 mV when 80 ppm of Ca is added. At pH 4, the zeta potentials for 40 and 80 ppm of Ca

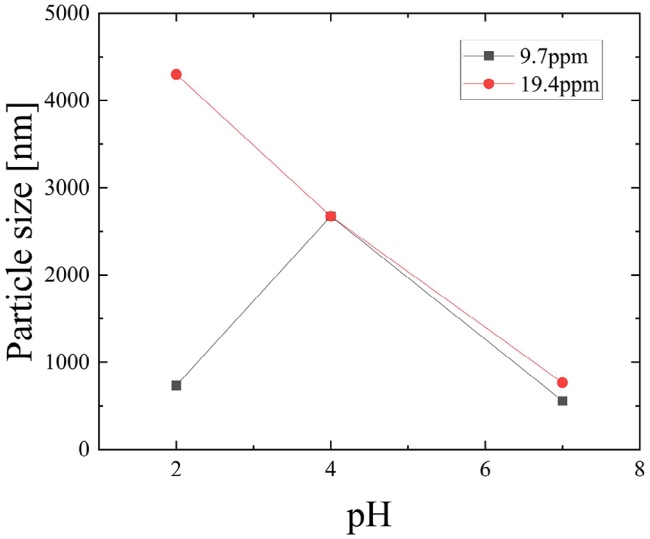

FIGURE 7 Particle size at different Mg concentrations.

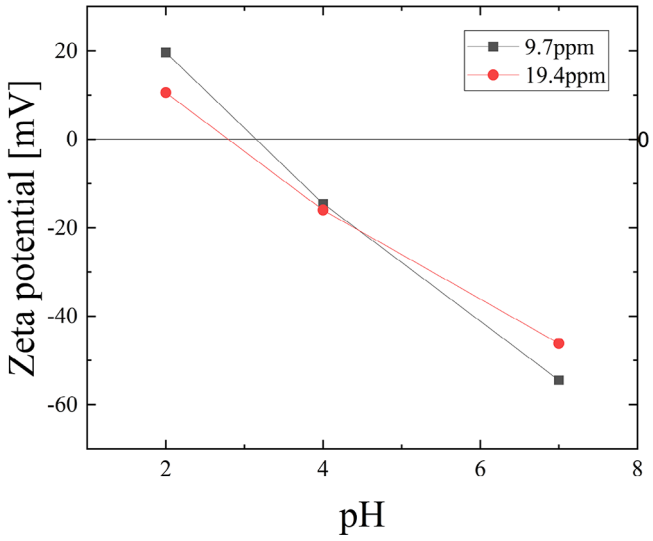

FIGURE 8 Zeta potential at different Mg concentrations.

are −17.28 and −5.18 mV, respectively. The zeta potential affects particle aggregation. Particularly, as the zeta potential approaches the equipotential point, the particles simultaneously approach the aggregate state. Regardless of whether the zeta potential is positive or negative, the greater the absolute value, the stronger the repulsion between particles. This indicates that at pH 4, the interparticle repulsion according to the DLVO theory is weakened with the increasing concentration of Ca. This is consistent with the appearance of the peak particle size at pH 4 (Figure 5). The increasing concentration of Ca is considered to have decreased the repulsion between particles at pH 4, thereby facilitating electrostatic aggregation. In addition, the increase in the particle diameter at pH 4 is attributed to the flocculating effect of Ca.

In this study, the addition of Ca ions is considered to cause co-precipitation, as in the case of Al-ion addition. This is also evident from the increase in the average particle size with the increasing concentration of the added Ca (Figure 3). Furthermore, the particle size is affected by the changes in the pH, owing to the simultaneous variation in the zeta potential between the particles, which consequently alters the cohesive force between the particles.

3.3 | Effect of Mg addition on zeta potential and particle size

Figure 7 shows the particle size distribution at different levels of Mg-ion addition. When the Mg-ion concentration is 9.7 ppm, the peak particle size is observed at pH 4. Additionally, the particle size increases at pH 2 when the concentration of the added Mg is increased to 19.4 ppm. Considering silica removal performance, Sheikholeslami et al.[21] stated that Mg ions flocculated and precipitated silica; they observed that adding magnesium hydroxide to aqueous solutions containing silica effectively removed silica from the solutions.

According to Zhang et al.[22], the presence of divalent ions in aqueous colloidal solutions strongly affects colloidal aggregation and reduces the thickness of the electric double layer on the colloidal surface. This is because the divalent metal ions neutralize the negative charges on the colloidal surface. This reduced thickness of the electric double layer enables colloidal particles to approach and bond with each other. Consequently, the bonding between colloids is promoted, and the rate of aggregation is rapidly increased.

Figure 8 shows that the zeta potential does not substantially change with increasing Mg content. This is possibly because the concentration of Mg added is lower than that used in the Ca experiment. As shown in Figure 7, the particle size at pH 4 does not increase with the increasing Mg content. Furthermore, at pH 4, the zeta potentials for 9.7 and 19.4 ppm of Mg are −14.54 and −16.0 mV, respectively (Figure 8); the difference between these zeta potentials (1.46 mV) is insignificant.

The zeta potential value at pH 2 decreases from 19.64 mV at 9.7 ppm of Mg to 10.56 mV at 19.4 ppm of Mg. The results indicate that the zeta potential approaches the equipotential point with increasing Mg addition. Figure 7 depicts an increase in the particle size at pH 2, which is consistent with the results presented in Figure 8, because the zeta potential approaches the equipotential point at pH 2, indicating a scenario where the cohesive force according to the DLVO theory is expected to be active.

In this study, the changes in the zeta potentials of Mg, a divalent cation, and Ca are ascribed to changes in pH. The

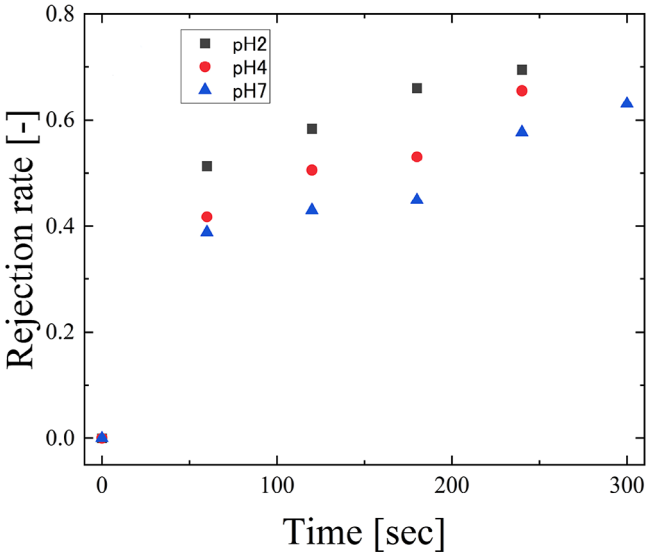

FIGURE 9 Removal rate at different pH values.

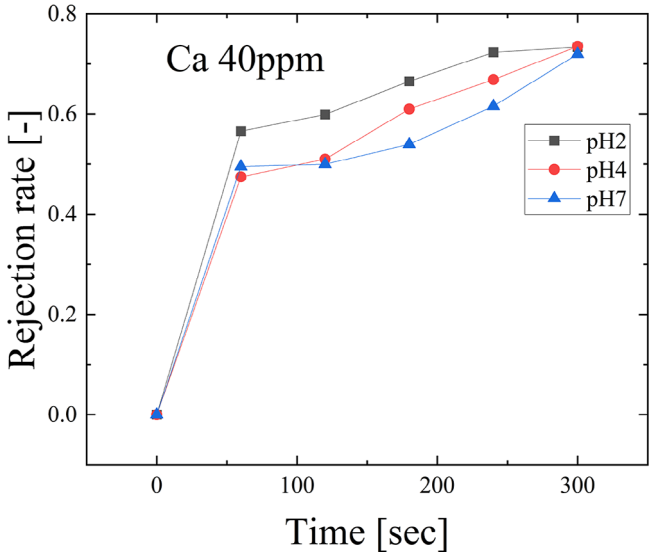

FIGURE 10 Removal rate of 40 ppm Ca at different pH values.

resulting change in particle cohesion possibly increases the average particle size at pH 2.

3.4 | Sliding test at different pH values without cation addition

The removal rate R of the silica scale is defined as follows:

$$R = 1 - V/V_0, \tag{2}$$

where V_0 is the initial volume of the silica scale, and V is the volume of the scale 60 min after the sliding test.

Figure 9 shows the results of the sliding tests of water stains formed by silica-containing water at pH values of 2, 4, and 7 with 0% Al addition. The progress of silica-scale removal by sliding is observed: the volume of the silica scale decreases with increasing sliding time at all pH values. The removal rate of the silica scale increases with decreasing pH. According to Choppin et al.,[23] silica-scale polymerization was enhanced at higher pH. However, in this study, SiO_2 precipitated as a silica scale upon drying, but the silica spheres did not polymerize in the low-pH region. Consequently, the bonds between the silica spheres weakened, and the bulk scale became more brittle, thereby increasing the removal rate.

3.5 | Change in water-stain volume at different pH values and Ca concentrations

Figures 10 and 11 show the changes in the volume and removal rates of water stains upon adding different concentrations of Ca. As described in Section 3.4,

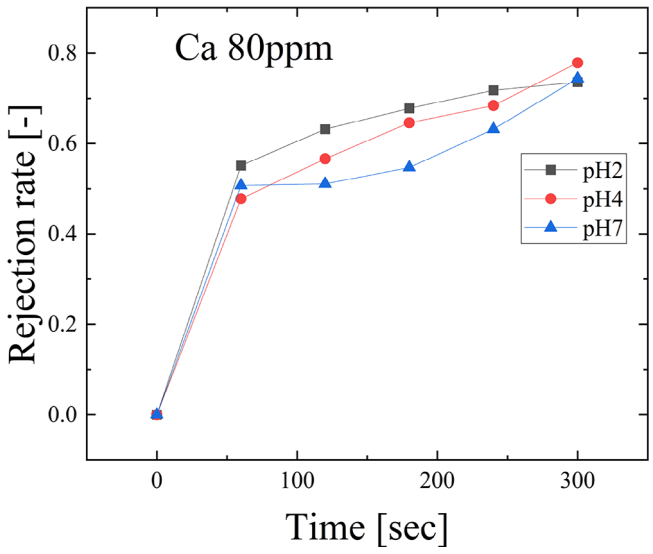

FIGURE 11 Removal rate of 80 ppm Ca at different pH values.

the behavior of silica is affected by both its pH and propensity for polymerization. In this experiment, with the addition of Ca, the water-stain volume decreased more rapidly at a lower pH, resulting in a higher removal rate at a lower pH. This trend did not change when the amount of added Ca was varied from 40 to 80 ppm. The trend of the removal rate with respect to the pH was found to be identical to that in the absence of Ca, as described in Section 3.4. Thus, water stains were easier to remove at a lower pH, possibly because silica polymerization did not proceed in the low-pH range (Section 3.4).

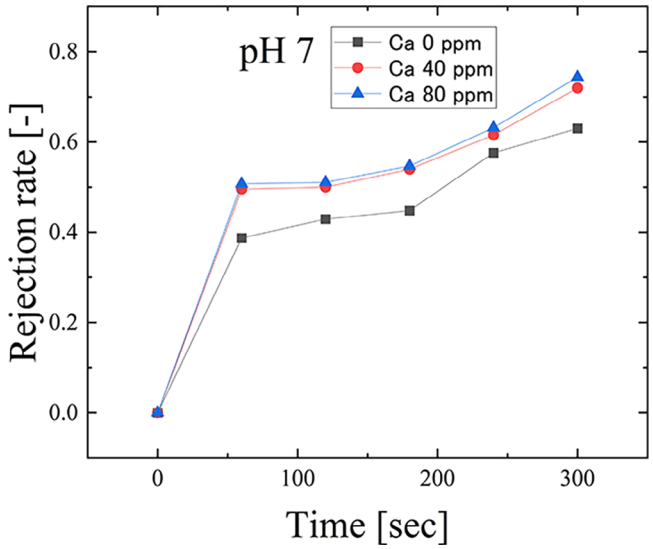

FIGURE 12 Removal rate at 7 pH for various Ca concentrations.

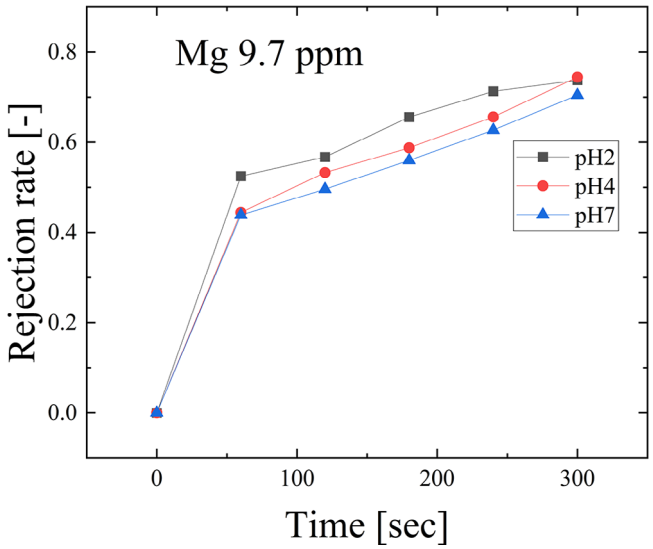

FIGURE 13 Removal rate of 9.7 ppm Mg at different pH values.

3.6 | Sliding tests with varying concentrations of Ca

Figure 12 shows the silica-scale removal rates for different Ca concentrations. The samples with added Ca exhibit higher water-stain removal rates than that without added Ca. The final removal rate of the 0 ppm Ca sample at pH 7 is 0.63 after 300 s of sliding, whereas those of the 40 and 80 ppm Ca samples are 0.71 and 0.74, respectively. These results suggest that the addition of Ca facilitates water-stain removal.

Chen et al.[24] reported that in a system containing Na, Si, and calcium nitrate, the SiO_2–H_2O system (C–S–H) was synthesized and precipitated. C–S–H is the generic term for crystalline calcium silicate hydrates, which exhibit more than 30 structures and morphologies, ranging from semi-crystalline to amorphous. In their study, 0.050 mol of $Na_2SiO_3{\cdot}5H_2O$ was dissolved in 125 mL of deionized water. Deionized water containing 0.075 mol of $Ca(NO_3){\cdot}4H_2O$ was added to this solution to obtain the C–S–H compound. Their study is fundamentally similar to the present study, as both involve the ionization of Na when incorporated into an aqueous solution, despite the difference in the starting material, which was $Na_2SiO_3{\cdot}5H_2O$ in their study.

In this study, as shown in Figure 5, the particle size increased with increasing Ca concentration. A larger particle size was expected to result in a coarser water-stain structure after drying. The sliding results were considered to be affected by the formation of a compound resulting from the addition of Ca and by the increase in particle size and consequent coarse structure of the water stain. We assume that C–S–H was produced in the present study,

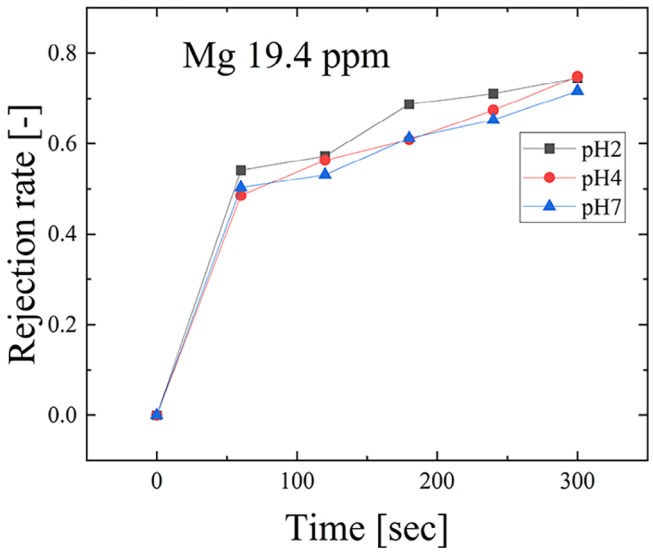

FIGURE 14 Removal rate of 19.4 ppm Mg at different pH values.

as in the study conducted by Chen et al.[24] The generated C–S–H was possibly mixed as colloidal silica and agglomerated to form bulk silica. Coagulation and precipitation were expected to have produced relatively large sediments, forming water stains with coarse structures. This indicated that the water stains were weakened by the addition of Ca.

3.7 | Change in water-stain volume at different pH values and Mg concentrations

Figures 13 and 14 show the changes in the volume and removal rate of water stains upon adding different

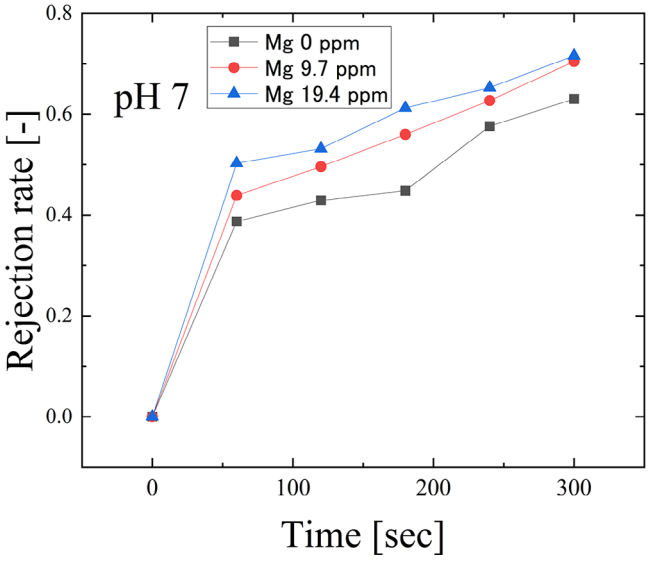

FIGURE 15 Removal rate at 7 pH for various added Mg concentrations.

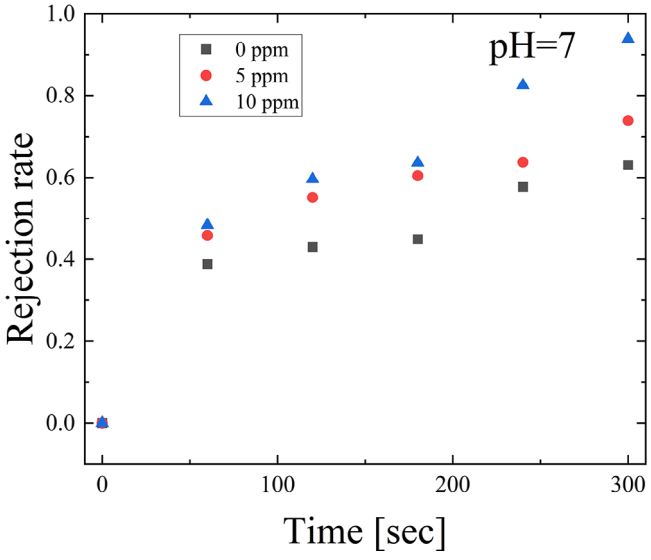

FIGURE 16 Removal rate at 7 pH for various added Al concentrations.

concentrations of Mg. The water stains were removed as sliding progressed. Similar to the addition of Ca, low pH values increased the effectiveness of water-stain removal. Samples with lower pH were easier to remove by sliding.

In this experiment, the ease of water-stain removal in a low-pH environment is identical to that described in Section 3.4. Considering that the concentration of added Mg is less than that of Ca, the results are expected to be similar to those described in Section 3.4 with no cation addition. Consequently, the overall water-stain behavior is expected to be consistent with that of water stains without cations at this level of Mg addition, primarily because the removal rate is high at low pH.

3.8 | Sliding tests with varying concentrations of Mg

Figure 15 shows the volume change and water-stain removal rates for different concentrations of Mg. As the Mg concentration is increased, the water-stain volume decreases and the removal rate increases. After 300 s of the sliding test, the 9.7 and 19.4 ppm Mg samples exhibit removal rates that are 1.12 and 1.14 times higher than that of the 0 ppm Mg sample, respectively.

Magnesium silicate possibly precipitated in this study, similar to the observation by Krysztafkiewicz et al.[25] They reported that magnesium silicate precipitated when sodium silicate and magnesium nitrate were dissolved and stirred in an aqueous solution. A precipitate (magnesium silicate) was obtained by reacting an aqueous solution of sodium metasilicate with a concentration of 5% SiO_2 and an aqueous solution of 5% magnesium nitrate. Although the initiators used in the present study were different, the similarities between the two studies include the involvement of sodium ions and monomeric silica in the aqueous solutions. We speculate that magnesium silicate precipitated into the aqueous solution in the present study. Comparing the samples with 9.7 and 19.4 ppm Mg, the water-stain removal rate increased with the increasing concentration of the added Mg.

The above-mentioned factors are expected to cause precipitation in the solution and increase the particle size. Thus, the water stain adopts a coarse structure with voids, and the removability is improved.

3.9 | Sliding tests with varying concentrations of Al

Figure 16 shows the results of sliding tests on the samples prepared at pH 7 with different Al concentrations. Sliding at all Al concentrations decreases the silica-scale volume, indicating that removal progresses. The silica-scale volume does not approach zero, suggesting that the sliding test for 300 s removes the surface of the silica scale, but not the bottom, which adheres to the substrate. As described in Section 3.1, kaolinite is assumed to be formed via co-precipitation. Regarding the strength of the bonds between kaolinite particles co-precipitated during the droplet drying process, Ichikuni[26] reported the presence of hydroxyl groups on the surface of clay (kaolinite) when mixed with water. As it dried, weak bonds were formed between kaolinite particles, as indicated by the dotted lines in Figure 17. This weak bond connects the kaolinite particles. The kaolinite precipitated in this study and the sediments

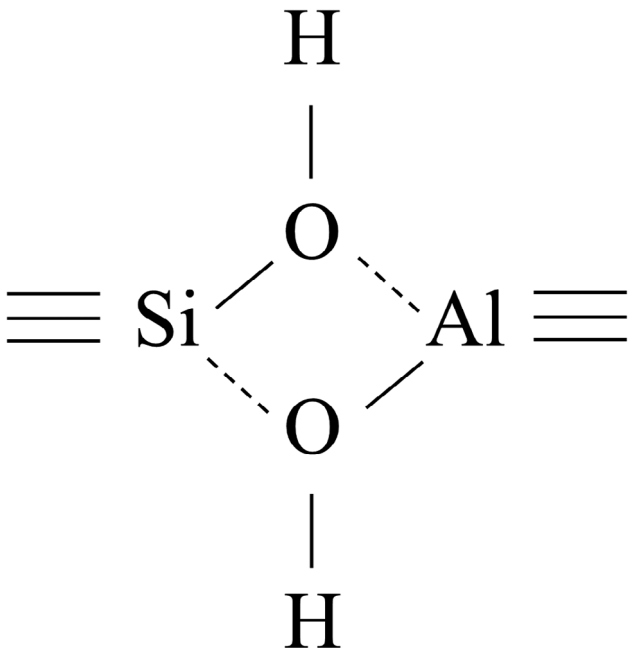

FIGURE 17 Weak bonding after clay is dried.[26]

when the water finally dried were kaolinite bound to kaolinite by weak bonds.[26] Furthermore, Ichikuni stated that clay kneaded with water solidifies upon drying. This implies that the particles are bound together by a certain force. Hardened clay is not tough and can be crushed easily because of weak forces acting between the particles or a small number of bonds linking the particles together. When water is poured onto the hardened clay, its shape collapses rapidly. Therefore, the bonds between the particles are sufficiently weak to be broken by water.

Particularly, as water dries, weak bonds are formed between kaolinite particles; however, because water is used in the sliding test, these bonds are expected to be easily broken. Based on the above-mentioned findings, the following can be inferred:

(1) Some silica particles co-precipitate to form kaolinite.
(2) Weak bonds are formed between kaolinite particles by drying.
(3) The weak bonds are easily broken by water during sliding.

These three observations suggest that the entire silica scale can be easily removed by water during sliding.

3.10 | Discussion on cohesive phenomena

In this study, cullet samples were produced by melting sodium carbonate (Na_2CO_3) and silicon dioxide (SiO_2) at high temperatures. The molar masses of sodium carbonate and silicon dioxide are 105.99 and 60.08 g/mol, respectively. Accordingly, 4 g = 3.77×10^{-2} mol of sodium carbonate, and 1 g = 1.66×10^{-2} mol of silicon dioxide. The reaction for the preparation of a sodium silicate cullet is as follows:

$$Na_2CO_3 + nSiO_2 \rightarrow Na_2O \cdot nSiO_2 + CO_2 \quad (3)$$

The value of n is obtained from the molar ratio of Na_2CO_3 and SiO_2 in this study; $n = 1.66 \times 10^{-2}/3.77 \times 10^{-2} = 0.44$, suggesting that n is less than 1 and that excess unreacted Na is present in the aqueous solution. Assuming that 1.66×10^{-2} mol of sodium silicate is produced at $n = 1$ and the remaining Na is retained in the aqueous solution in the form of unreacted Na ions, the amount of unreacted Na in the aqueous solution can be calculated as follows:

$$\text{Unreacted Na} = \left(3.77 \times 10^{-2} - 1.66 \times 10^{-2}\right)/2 = 1.055 \times 10^{-2}\,[\text{mol}] \quad (4)$$

When a cullet of soda carbonate is dissolved in water, it becomes alkaline; however, the pH essentially depends on the amount dissolved.[27] The overall weight of 1.66×10^{-2} mol of sodium silicate is 4.58 g. The sodium silicate content (wt%) in the aqueous solution is calculated as follows: wt% = 4.58/1000 = 4.58×10^{-3} wt%. Based on the study by Hamouda and Akhlaghi Amiri,[27] the lowest point on the graph is 0.02 wt%, and the pH is 10.13; therefore, the initial pH in this study is similar to or below this value. Kim et al.[28] reported that in aqueous solutions containing silica particles and distilled water, the zeta potential decreases with increasing pH. The zeta potentials of other inorganic oxide particle systems have also been reported to decrease with increasing pH, indicating that this trend is somewhat common.[29–31] Figures 4, 6, and 8, which depict the change in zeta potential upon Al, Ca, and Mg addition, respectively, present similar trends. The zeta potential shifts with the change in pH, and approaches the equipotential point at a specific pH (e.g., pH 4 in the Al addition experiment; Figure 4).

The dispersion of a group of particles in an aqueous solution depends on the surface charge.[32,33] A layer of charge, called an electric double layer, is formed on the surface of the particles in an aqueous solution. This electric double layer is formed when the surface of a particle suspended in a liquid accumulates an electric charge that is the opposite of the surface charge of the particle. The plane in which the particles do not move through the solution is called the slipping plane, and the potential of this plane is defined as the zeta potential. Hanaor et al.[34] studied the aggregation of ZrO_2 dispersed

in an aqueous solution and described the aggregation of inorganic particles at the point where the zeta potential became zero, that is, the equipotential point. Positively or negatively charged solutions are more stable as colloids in colloidal suspensions. When the absolute value of the zeta potential is high, the particles are uniformly dispersed, and sedimentation is prevented. However, as the zeta potential approaches the equipotential point, van der Waals forces become dominant over the electrostatic repulsive forces between the particles, causing them to gradually approach each other and eventually agglomerate. In this study, the maximum particle diameter was observed at the equipotential point, indicating that the electrostatic repulsion between the particles had weakened.

3.11 | Discussion on bulk strength of water stains

In the present study, the removability of water stains is improved under the influence of all added ions (Al, Ca, and Mg). The increase in the particle size of the water stain is regarded as one of the factors contributing to the improved removability. The water stains are composed of numerous silica spheres.[35] Therefore, the bonding between the silica spheres is considered to determine the strength of the bulk. Based on the particle size measurements, precipitates are formed in the aqueous solution in this study. We assume that this increase in particle size causes the water stain to become brittle. In this study, the water stain destroyed in the sliding test can be regarded as a type of floc in which the precipitates in the aqueous solution agglomerate to form the bulk. According to Matsuo,[36] the floc density increases with the increasing floc particle size; however, the bulk porosity simultaneously increases. This decreases the number of bonds between the basic particles that constitute the floc per unit volume, and consequently decreases the strength. In the present study, the number of contacts per unit volume between particles is considered to decrease with the increasing diameter of the particles constituting the water stain, considering that the water stain is easily removed by sliding.

4 | CONCLUSIONS

Artificial silica-based water stains were created on a glass surface to mimic the practical system, and the addition of Ca and Mg was found to improve the silica-scale removal rate. In this study, we confirmed that the addition of divalent ions caused a flocculation/co-precipitation effect. The entire water stain was made more fragile by the formation of precipitates containing Ca and Mg rather than silica alone. The addition of various cations was considered to produce precipitates during water staining. A larger particle size enhanced water-stain removal because of the sparse structure of the entire water stain. However, the composition of the sediments was not analyzed in this study; therefore, the sediments must be subjected to x-ray diffraction analysis to test this hypothesis. Sliding tests at different pH values indicated that silica polymerization became more challenging in the low-pH region. As polymerization did not proceed, bonds between the silica particles were not formed, and the water-stain structure was weak. In the tests with added Al, silica-scale removal was facilitated at higher Al concentrations owing to the formation of kaolinite as a precipitate and the weak bonding in the dried kaolinite.

This study revealed that adding cations to water increased the brittleness of the water stains. This weakening of the water stains helps to improve the cleanliness of sanitary ware, because it reduces the frequency of sanitary ware maintenance, inhibits mold, and prevents other problems caused by water stains.

ORCID

Shogo Hayashi https://orcid.org/0000-0003-0381-6825

REFERENCES

1. Huuhtanen S, Laukkanen A. A guide to sanitation and hygiene for those working in developing countries. Tampere, Finland: University of Applied Sciences Publications Tampere; 2006.
2. Abney SE, Bright KR, McKinney J, Ijaz MK, Gerba CP. Toilet hygiene—review and research needs. J Appl Microbiol. 2021;131:2705–14. https://doi.org/10.1111/jam.15121
3. Sunarsa IW, Andiani ND. Tourism perception of general toilet hygiene in objects and tourist attractions in Bali. Int J Soc Sci Business. 2019;3:28–35. https://doi.org/10.23887/ijssb.v3i1.17162
4. Wang J, Wang L, Sun N, Tierney R, Li H, Corsetti M, et al. Viscoelastic solid-repellent coatings for extreme water saving and global sanitation. Nat Sustain. 2019;2:1097–105. https://doi.org/10.1038/s41893-019-0421-0
5. Powell JJ, McNaughton SA, Jugdaohsingh R, Anderson SHC, Dear J, Khot F, et al. A provisional database for the silicon content of foods in the United Kingdom. Br J Nutr. 2005;94:804–12. https://doi.org/10.1079/BJN20051542
6. McCartney TR, Gharaibeh S, Shank R. Improved methods for removal of silicate deposits. In: Heat exchanger fouling and cleaning. XII. 2017. p. 235–39.
7. Neofotistou E, Demadis KD. Use of antiscalants for mitigation of silica (SiO_2) fouling and deposition: fundamentals and applications in desalination systems, Desalination. 2004;167:257–72. https://doi.org/10.1016/j.desal.2004.06.135
8. Amjad Z, Yorke MA. Carboxylic functional polyampholytes as silica polymerization retardants and dispersants. U.S. Patent No. 4,510,059. United States Patents; 1985.
9. Harrar JE, Lorensen LE, Locke FE. Method for inhibiting silica precipitation and scaling in geothermal flow systems. U.S. Patent No. 4,328,106. United States Patents; 1982.

10. Spinthaki A, Kamaratou M, Skordalou G, Petratos G, Tramaux A, David G, et al. A universal scale inhibitor: a dual inhibition/dispersion performance evaluation under difficult brine stresses. Geothermics. 2021;89:101972. https://doi.org/10.1016/j.geothermics.2020.101972
11. Gallup DL. Investigations of organic inhibitors for silica scale control in geothermal brines. Geothermics. 2002;31:415–30. https://doi.org/10.1016/S0375-6505(02)00004-4
12. Gill JS. Inhibition of silica–silicate deposit in industrial waters. Colloids Surf A: Physiochem Eng. 1993;74:101–6. https://doi.org/10.1016/0927-7757(93)80401-Y
13. Ministry of Education, Culture, Sports, Science, and Technology. Inorganic matter in tap water. Ministry of Education, Culture, Sports, Science, and Technology. https://www.mext.go.jp/component/a_menu/ (accessed November 7, 2023)
14. Deegan RD, Bakajin O, Dupont TF, Huber G, Nagel SR, Witten TA. Capillary flow as the cause of ring stains from dried liquid drops. Nature. 1997;389:827–29. https://doi.org/10.1038/39827
15. Dugyala VR, Basavaraj MG. Control over coffee-ring formation in evaporating liquid drops containing ellipsoids. Langmuir. 2014;30:8680–86. https://doi.org/10.1021/la500803h
16. Bhardwaj R, Fang X, Somasundaran P, Attinger D. Self-assembly of colloidal particles from evaporating droplets: role of DLVO interactions and proposition of a phase diagram. Langmuir. 2010;26:7833–42. https://doi.org/10.1021/la9047227
17. Sheikholeslami R, Al-Mutaz IS, Koo T, Young A. Pretreatment and the effect of cations and anions on prevention of silica fouling. Desalination. 2001;139:83–95. https://doi.org/10.1016/S0011-9164(01)00297-1
18. Tokoro C, Suzuki S, Haraguchi D, Izawa S. Silicate removal in aluminum hydroxide co-precipitation process. Materials. 2014;7:1084–96. https://doi.org/10.3390/ma7021084
19. Zuhl RW, Amjad Z. Solution chemistry impact on silica polymerization by inhibitors. In: Mineral scales in biological and industrial systems. Boca Raton, FL: CRC Press; 2013. p. 174–97.
20. Amjad Z, Zuhl RW. The role of water chemistry on preventing silica fouling in industrial water systems. Paper presented at: NACE Corrosion, 2010;10048.
21. Sheikholeslami R, Al-Mutaz IS, Tan S, Tan SD. Silica fouling—effect of Ca, Mg, and pretreatment by sodium aluminate, and softeners. Paper presented at: 6th World Congress in Chemical Engineering, Melbourne, Australia, 2001.
22. Zhang J, Li H, Li S, Hou X. Effects of metal ions with different valences on colloidal aggregation in low-concentration silica colloidal systems characterized by continuous online zeta potential analysis. Colloids Surf A. 2015;481:1–6. https://doi.org/10.1016/j.colsurfa.2015.04.024
23. Choppin GR, Pathak P, Thakur P. Polymerization and complexation behavior of silicic acid: a review. Main Group Met Chem. 2008;31:53–72. https://doi.org/10.1515/MGMC.2008.31.1-2.53
24. Chen JJ, Thomas JJ, Taylor HFW, Jennings HM. Solubility and structure of calcium silicate hydrate. Cem Concr Res. 2004;34:1499–519. https://doi.org/10.1016/j.cemconres.2004.04.034
25. Krysztafkiewicz A, Lipska LK, Ciesielczyk F, Jesionowski T. Amorphous magnesium silicate—synthesis, physicochemical properties and surface morphology. Adv Power Technol. 2004;15:549–65. https://doi.org/10.1163/1568552042000183
26. Ichikuni M. Naze nendo wa katamaruka [Why clay hardens]. Kagaku Kyouiku [Chem Educ]. 1995;43:558–61. https://doi.org/10.20665/kakyoshi.43.9_558
27. Hamouda AA, Akhlaghi Amiri HA. Factors affecting alkaline sodium silicate gelation for in-depth reservoir profile modification. Energies. 2014;7:568–90. https://doi.org/10.3390/en7020568
28. Kim I, Taghavy A, DiCarlo D, Huh C. Aggregation of silica nanoparticles and its impact on particle mobility under high-salinity conditions. J Pet Sci Eng. 2015;133:376–83. https://doi.org/10.1016/j.petrol.2015.06.019
29. Hemati A, Shrestha S, Agarwal M, Varahramyan K. Layer-by-layer nanoassembly of copper indium gallium selenium nanoparticle films for solar cell applications. J Nanomater. 2015;2012:512409. https://doi.org/10.1155/2012/512409
30. Cieslik I, Węglowski R, Żmija J, Kurzydłowski K, Płocińska M, Oćwieja M. Control of optical active borates nanocrystals agglomeration. J Achiev Mater Manuf Eng. 2014;61:163–68.
31. Zarbov M, Brandon D, Cohen N, Shemesh L. Engineering performance in applied EPD: problems and solutions. J Mater Sci. 2006;41:8115–22. https://doi.org/10.1007/s10853-006-0418-8
32. Sarkar P, Nicholson PS. Electrophoretic deposition (EPD): mechanisms, kinetics, and application to ceramics. J Am Ceram Soc. 2002;79:1987–2002. https://doi.org/10.1111/j.1151-2916.1996.tb08929.x
33. Will J, Hruschka MKM, Gubler L, Gauckler LJ. Electrophoretic deposition of zirconia on porous anodic substrates. J Am Ceram Soc. 2001;84:328–32. https://doi.org/10.1111/j.1151-2916.2001.tb00658.x
34. Hanaor D, Michelazzi M, Leonelli C, Sorrell CC. The effects of carboxylic acids on the aqueous dispersion and electrophoretic deposition of ZrO_2. J Eur Ceram Soc. 2012;32:235–44. https://doi.org/10.1016/j.jeurceramsoc.2011.08.015
35. Hayashi S, Kobayashi T, Saito N, Nakashima K. Coffee-ring-effect-induced water scale formation of silicic acid-containing droplet. Int J Ceram Eng Sci. 2020;2:228–33. https://doi.org/10.1002/ces2.10059
36. Matsuo T. Breakup and strength of floc. Paper presented at: Proceedings of the Japan Society of Civil Engineers, 1974:31–39. https://doi.org/10.2208/jscej1969.1974.229_31

How to cite this article: Hayashi S, Hatano S, Kobayashi T, Saito N, Nakashima K. Effect of cation addition on silica scale on glass surfaces. Int J Ceramic Eng Sci. 2024;6:e10203. https://doi.org/10.1002/ces2.10203